

JOHNSON  
GRANT

1N-20-CR

187643

31P

Grant No. NAG9 - 201

# INVESTIGATION OF ENERGY TRANSFER IN THE IGNITION MECHANISM OF A NASA STANDARD INITIATOR

Final Technical Report

For the Period

February 1, 1987 - August 1, 1988

Submitted by

Dr. Philip L. Varghese

The University of Texas at Austin

Department of Mechanical Engineering

Austin, TX 78712

(NASA-CR-184673) INVESTIGATION OF ENERGY  
TRANSFER IN THE IGNITION MECHANISM OF A NASA  
STANDARD INITIATOR Final Technical Report, 1  
Feb. 1987 - 1 Aug. 1988 (Texas Univ.) 31 p

N89-15169

Unclas

CSC L 21H G3/20 0187643

Grant No. NAG9 - 201

INVESTIGATION OF ENERGY TRANSFER IN THE IGNITION  
MECHANISM OF A NASA STANDARD INITIATOR

Final Technical Report

For the Period

February 1, 1987 - August 1, 1988

Submitted by

Dr. Philip L. Varghese

The University of Texas at Austin

Department of Mechanical Engineering

Austin, TX 78712

## TABLE OF CONTENTS

1.	Summary .....	1
2.	Introduction .....	2
3.	Summary of Previous Work .....	2
4.	Current Work .....	8
5.	Conclusions .....	24
6.	References.....	26
Appendix		
	Curvefits to Thermophysical Properties .....	27

## 1. SUMMARY

The principal objective of the proposed research was to construct a detailed computer model of the NASA Standard Initiator (NSI). The NSI plays a critical role in initiating various pyrotechnic events in the National Space Transportation System and is also used in Shuttle payload applications. Several initiators failed when being tested at very low temperatures (4 - 20 K). During subsequent investigation an unacceptably high failure rate was found even at higher temperatures (100 - 150 K) but the precise cause of failure was not determined. The modelling work was undertaken to investigate reasons for failure and to predict the performance of alternate firing schemes. The work has shown that the most likely cause of failure at low temperature is poor thermal contact between the electrically heated bridgewire and the pyrotechnic charge. This problem may be masked if there is good thermal contact between the bridgewire and alumina charge cup. The high thermal conductivity of alumina at cryogenic temperatures was overlooked in previous analyses, which assumed that the charge cup acted as a thermal insulator.

### 3. INTRODUCTION

The NASA Standard Initiator (NSI) shown in Fig. 1 is an electrochemical device which plays a critical role in initiating various pyrotechnic events in the National Space Transportation System. It is also used for Shuttle payload applications. The NSI is activated by electrically heating a thin metal bridgewire lying at the bottom of a small alumina cup. The bridgewire is surrounded by a pyrotechnic charge of zirconium potassium perchlorate (ZPP) which fills the cup. Energy transfer from the bridgewire to the ZPP pellet causes it to ignite and a chemical chain reaction results in a small detonation. The resulting high pressures may be used directly to actuate small components or to initiate reactions in larger explosive charges.

Recently several initiators from a certain production lot failed when being tested at very low temperatures (21 K). During subsequent investigation an unacceptably high failure rate was found even at higher temperatures (144 K). Some batches from other lots that had previously been accepted also failed the tests. Extensive testing and some numerical modelling failed to pinpoint the cause of failure at low temperatures.<sup>1</sup> This work is briefly described in the following section. The modelling undertaken in this work and numerical results are described in Section 4. In the final section future work to be conducted under an additional grant is outlined.

### 3. SUMMARY OF PREVIOUS WORK

When the high failure rate of initiators at low temperature was discovered an extensive investigation was initiated to determine the reason for failure. This work was undertaken at NASA Johnson Space Center, and Hi Shear Corporation of Torrance, California with consulting support from other NASA Centers, other government agencies, and commercial organizations.

#### Scanning Electron Microscopy and Energy Dispersive Spectroscopy

These tests were made to determine if charge contamination or morphology varied between lots that had a high failure rate and those that experienced no failures. A scanning electron microscope was used to examine the NSI pyrotechnic charges. Some differences in mix morphology (particle size, shape, and size distribution) were found between lots from different suppliers but there was no correlation between the firing performance and the morphology of the charge. When charge samples from some failed initiators were examined, it was noticed that the potassium perchlorate ( $\text{KClO}_4$ ) at the wire/charge interface had fused. Since  $\text{KClO}_4$  begins to

# NASA STANDARD INITIATOR, TYPE 1 (NSI-1)

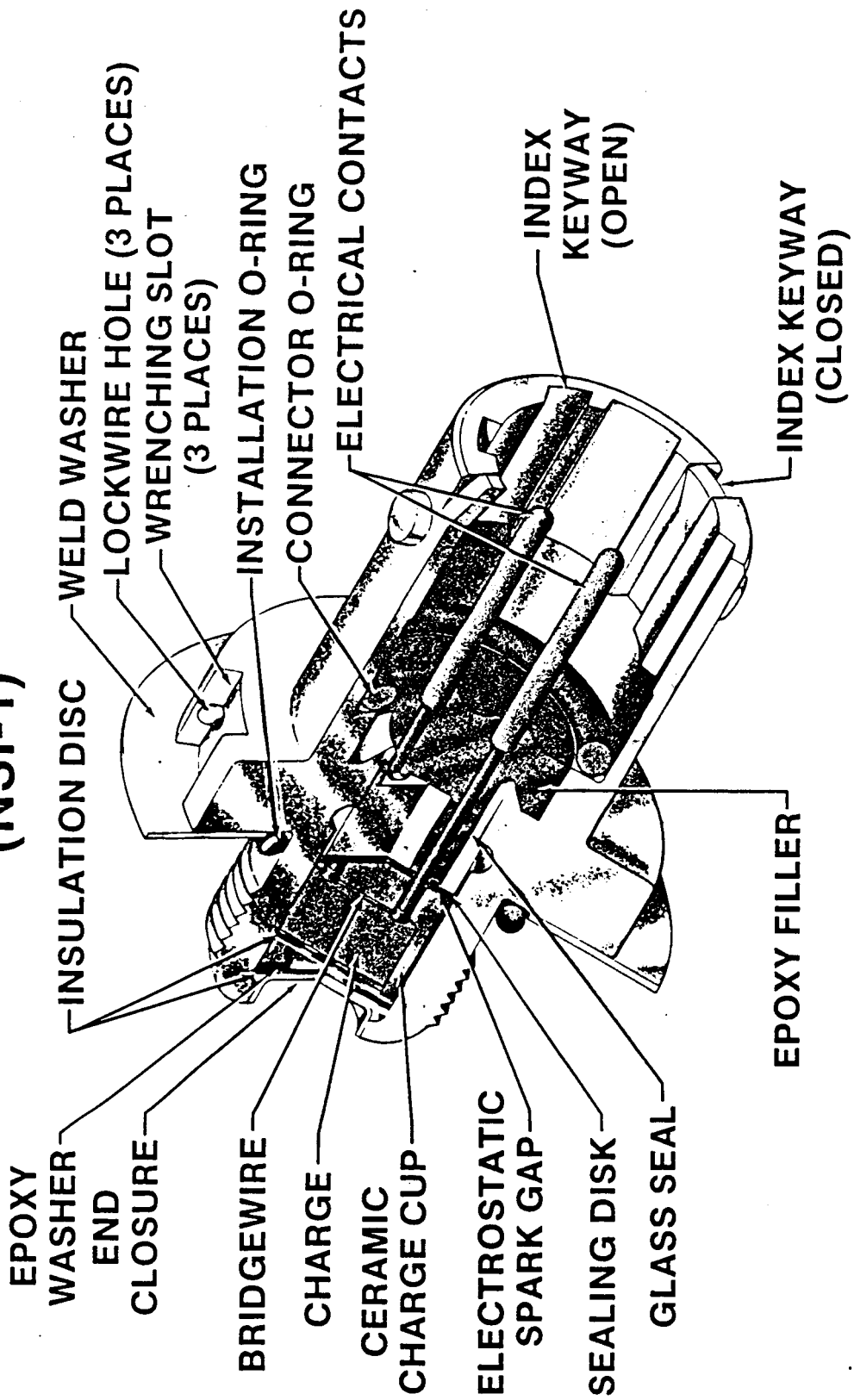


Figure 1 Sectional view of NASA Standard Initiator

decompose at temperatures below its melting point it was concluded that reaction had been initiated in these initiators but that a self-propagating condition was not achieved.

Charges from initiators that failed to ignite, as well as some which were not yet tested for ignition, were examined using energy dispersive spectroscopy. It was found that some charge samples were contaminated, but the trace quantities of silicon, iron, and chromium detected would have no effect on the initiator performance. It was also concluded that the contaminants were probably introduced into the samples while removing the charge from the initiators.

### Zirconium Oxidation Level

The objective of this test was to determine if the oxidation level of zirconium affected the sensitivity of the charge. Because zirconium is a very sensitive metal, it is shipped, delivered, and stored in an aqueous solution. Before being mixed with potassium perchlorate, the zirconium is dried in an oven while exposed to air. The drying procedure was not tightly controlled between samples: drying temperature varied from 65° to 93°C, and drying time varied from a few hours to several days. It was thought that the extended drying time at higher temperatures might lead to surface oxidation of the zirconium and make it harder to ignite. Four samples from each of the three different suppliers of zirconium were subjected to various drying conditions, and then tested for oxidation. The results showed that even though the oxidation level increased with the time of exposure, the changes in oxidation levels of the various samples were negligible. It was concluded that variation of the drying parameters did not have a significant effect on the sensitivity of the pyrotechnic charge.

### Zirconium Sources

This test was conducted to determine if zirconium samples from different suppliers experienced different behavior when test fired after being mixed with potassium perchlorate and loaded in the NSI. Zirconium from one vendor had shown excellent ignition performance at low temperatures in some lots, but the highest failure rate (85% failure at 22 K) in another lot. Supplies from two vendors were used to make new lots of initiators and tested at 22 K. Comparable ignition performance was obtained. It was thus concluded that zirconium was not the source of the problem.

### Reconsolidation Test and Pellet Expulsion Test

It was postulated that the charge pellet was contracting away from the bridgewire and walls of the charge cup and breaking free. A series of tests were conducted in which the pellet was forced against the bridgewire by placing a dead weight on it. An 8 gram ram was loaded on the charge face, and the initiators were test fired at 22 K. The failure rate experienced with the deadweight was comparable to that experienced without it at the same test temperature. Hence it was concluded that pellet did not break free at low temperatures.

Additionally, the force required to push the charge out of the alumina cup was measured at room temperature and liquid nitrogen temperature (294 K and 77 K). The results obtained at 77 K varied from 10 - 110 N (2 - 25 lbf), while results at 294 K varied from 90 - 190 N (20 - 42 lbf). The diminished force was consistent with differential contraction but since a force of at least 10 N (2 lbf) was required even at low temperature, it was concluded that the mixture could not be moving freely in the cup and pulling away from the bridgewire.

### Sealing Washer Test

The bonding strength of the sealing washers used by different manufacturers was tested. The bond strength of the epoxy used in the lots that failed at low temperatures was not diminished when cooled from room temperature to 77 K. It was concluded that the washers were not the cause of failure.

### Firing Mode

The objective of this test was to determine if the firing mode has an effect on the failure rate. The prototype initiators were tested (qualified) by firing them with a constant current of 5 A (CC mode). During a shuttle mission initiators are fired by the Pyrotechnic Initiator Controller, which consists of a 680  $\mu$ F capacitor charged to 38 V discharging into a nominal resistance of 1  $\Omega$  (PIC mode). The bridgewire resistance is originally 1  $\Omega$  and increases with temperature; the maximum resistance prior to melting is approximately 1.6  $\Omega$ . To simulate this firing mode initiators were requalified using a Standard Firing Unit consisting of a 1000  $\mu$ F capacitor charged to 20 V (SFU mode). The PIC firing mode had the highest failure rate: 85% at 22 K, and the SFU and CC firing modes had comparable failure rates at 22 K (40 and 42% respectively).

The bridgewire destruct times measured for the CC and SFU modes (~2ms at 21 K) were an order of magnitude larger than the destruct time for the PIC mode (0.2 - 0.4 ms at 21 K). It was



thought that smaller currents applied for longer times should deliver more energy than larger currents for shorter times, which might explain the improved performance with the CC and SFU firing modes. Since the wire destruct time was the shortest for the PIC mode, and since the maximum wire temperature is limited to the wire melting temperature, the PIC was expected to have the smallest energy delivery from the wire to the pyrotechnic charge. NASA set up instrumentation to measure current and voltage across the bridgewire and pins during firing so that the energy delivered to the wire could be measured for each firing mode. It was assumed that this energy was transferred from the wire to the charge mixture. The tests at 21 K showed that maximum energy was transferred in the bridgewire in the PIC mode (77 mJ), and the minimum in the CC mode (56 mJ). Hence the firing mode with the highest failure rate had the most energy transfer to the bridgewire. Therefore, it was concluded that increased energy delivery into the bridgewire (and hence the charge) much above the threshold required for firing did not improve the performance of the NSI. No satisfactory explanation could be found for the correlation of increased failure rate with a firing mode that increased energy transfer into the bridgewire.

#### Electrothermal Response Test

The objective of the Electrothermal Response Test (ETR) was to measure the thermal contact resistance between the wire and the charge mix. The test is performed by exciting the bridgewire with a small current for a short period of time and using the variation in the electrical resistance of the wire to monitor its temperature. Poor thermal contact leads to more rapid rise in wire temperature when heated. The power transfer coefficient,  $\gamma$  (W/K), measured in the test is the reciprocal of the thermal contact resistance between the wire and its surroundings. Initiators were tested using ETR at both ambient temperature and 77 K; the same units were then test fired at 21 K. The tests showed that thermal contact resistance increased at lower temperatures. This is expected because of differential thermal contraction. However two different lots with approximately the same mean value of  $\gamma$  (1256 and 1284  $\mu$ W/K) had dramatically different failure rates (0% and 85% respectively). Additionally, initiators within a given lot that failed did not have the lowest values of  $\gamma$ . It was thus concluded that increased thermal contact resistance between wire and charge was not the cause of failure. This inconclusive result was perhaps the most puzzling since inhibited energy transfer from bridgewire to charge mixture appeared to be the most logical reason for failure.

## Heat Transfer Analysis

A simple two-dimensional axisymmetric numerical model of the NSI was constructed to study transient heat transfer between the bridgewire and the mix and to determine the sensitivity of the NSI to the initial temperature of the system. Chemical reactions were not modelled and ignition was assumed to occur if the charge temperature reached 590 K. Thermophysical properties of the ZPP mixture were assumed constant independent of temperature. Temperature dependent specific heat and thermal conductivity of the bridgewire were included in the model. The axisymmetric model was justified on the basis that the alumina charge cup had negligible contact area with the bridgewire and was a good thermal insulator. Hence it was assumed to have little influence on initiator performance. The thermal conductivity of the charge mix was set at a nominal value of 24.9 W/m K (14.4 Btu/hr ft °F) at 100% packing density, which could be reduced or increased to allow for voids and uncertainty in property values. The model simulated the SFU and CC firing modes. The effect of thermal contact resistance was modeled by using a contact area factor that measured the "effective" contact area between the wire and the charge (uniformly distributed to preserve axial symmetry).

The model predicted ignition at all initial temperatures for contact area factors greater than  $10^{-6}$ . Such small contact areas were considered unlikely, implying that thermal decoupling of wire and charge was unlikely to be the cause of failure. Additionally, the measured bridgewire burnout times of initiators that failed corresponded to contact factors of about 60% in the model. With an initial temperature of 106 K, ignition times computed from the model ranged from 0.06 to 0.13 ms for the SFU firing mode depending on contact area factor and mixture thermal conductivity assumed. Bridgewire burnout times for this mode ranged from 0.13-0.62 ms for the cases studied. In the CC firing mode ignition times ranged from 1.24 to 1.67 ms and bridgewire burnout times varied between 1.7 and 5.7 ms. For a bridgewire completely insulated from the charge, burnout times were predicted to be 0.125 ms and 1.7 ms in the SFU and CC firing modes respectively. Experimental data at this initial temperature gave bridgewire burnout times in the range 0.36 - 0.66 ms for the SFU firing mode, and 4.42 - 6 ms for the CC firing mode. Initiators that failed to ignite in the SFU mode had comparable bridgewire burnout times (0.46 -0.64 ms). From these results it was concluded that thermal decoupling was not the cause of failure.

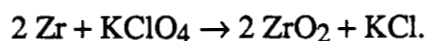
## 4. CURRENT WORK

In this section we describe the computer modelling and present the results obtained. The objective of the modelling was to determine the factors that led to successful ignition. This would identify possible failure modes particularly because a specific combination of temperature dependent properties appeared to be responsible for failure. Since many properties of an initiator can only be measured by destructive testing, there was little prospect of identifying the correct combination of factors experimentally without making measurements on a prohibitively large number of initiators.

### 4.1 One-dimensional (axisymmetric model)

In the first phase of this work we constructed a highly simplified one-dimensional axisymmetric model of the NSI. We assumed this simple model would reproduce the qualitative features of the ignition process. Heat transfer between bridgewire and charge mixture was assumed to occur by conduction only. Calculations showed that radiation heat transfer was likely to be insignificant because the bridgewire fused shortly after it became hot enough to radiate. The wire was assumed to be heated by a constant current of 5 A to simulate the CC firing mode.

This model was similar to the one described in the previous section but the following extensions were incorporated. The effect of differential thermal contraction was modelled by a thermal contact resistance between the wire surface and the charge mixture surrounding it. The variation of contact resistance with temperature was neglected. The use of a thermal contact resistance permitted the model to account for a temperature difference between wire surface and charge adjacent to it. Temperature gradients within the bridgewire were neglected. Energy release due to chemical reaction within the pyrotechnic charge was also included and the reaction was assumed to occur in a single step:



The chemical reaction rate was modelled by an Arrhenius type equation:

$$Z = A e^{(-E_a/RT)}$$

where  $Z$  is the reaction rate,  $A$  is a proportionality factor,  $E_a$  is the activation energy, and  $T$  is the absolute temperature. The rate of volumetric energy release,  $\dot{Q}$ , is

$$\dot{Q} = \rho Z \Delta H_R = \rho \Delta H_R A e^{(-E_a/RT)},$$

where  $\rho$  is the density of the mixture, and  $\Delta H_R$  is the enthalpy of reaction provided in the NSI-1 design and performance specifications (1395 cal/g mixture = 1870 MJ/kmol of  $KClO_4$ ).<sup>2</sup> Thermophysical properties were assumed to be constant for these calculations and many properties had to be estimated because data was not available at the time.

We developed our own computer code to solve the transient heat conduction problem because the packaged computer code we had available (PATRAN) could not handle variable time steps. These are required to resolve the rapid temperature rise that occurs once chemical reactions begin to release significant amounts of energy. We employed an explicit finite difference scheme which is forward in time centered in space (FTCS).<sup>3</sup> For this method to be stable, diffusion number  $\equiv \alpha \Delta t / (\Delta r)^2 \leq 1/2$ , where  $\alpha$  is the thermal diffusivity. We verified our code by comparing with results from PATRAN for the transient heat conduction problem with no chemical reactions.

Since the activation energy was not known, it was assumed to be  $0.13\Delta H_R$  (= 243 kJ/mol) for the base case and the pre-exponential factor, A, was set to  $1.82 \times 10^{17} \text{ s}^{-1}$ . This was found to give ignition at about 600 K in reasonable accord with experimental observations.<sup>4</sup> The thermal contact resistance between wire and charge inferred from differential thermal analysis measurements on samples of initiators varied between  $\sim 5 \times 10^{-5} \text{ m}^2 \text{ K/W}$  at 300 K to  $\sim 3 \times 10^{-4} \text{ m}^2 \text{ K/W}$  at 100 K.<sup>5</sup> As a base case the contact resistance was set at a low value of  $10^{-7} \text{ m}^2 \text{ K/W}$ . Table 1 summarizes the values of thermophysical properties used in the calculations.

Table 1 Properties used in Preliminary Calculation

Bridgewire Material: SS-304                      Diameter, D = 50  $\mu\text{m}$   
 ZPP charge:                      Stoichiometric composition (by weight) Zr: 0.568,  $KClO_4$ : 0.432

	SS 304	Zr	$KClO_4$	ZPP
Density ( $\text{kg/m}^3$ )	8030	6530	2500	4600
Specific Heat ( $\text{J/kg-K}$ )	500	280	200	250
Thermal Conductivity ( $\text{W/m-K}$ )	-	22.7	1*	13
Melting Temperature (K)	1700	-	-	-

\* No thermal transport data were found in a preliminary search. The value above is a crude estimate by analogy with similar compounds ( $KNO_3$ ,  $NH_4ClO_4$ ) for which data could be found.

Some results obtained with this simple model are presented in Figs. 2-4. On these figures the temperature of the bridgewire is shown with a dashed line, and the temperatures of the first two nodes within the ZPP are shown in solid lines. Each node in the charge represents a zone 60  $\mu\text{m}$  thick and zone temperature was calculated at the center of each zone. The zone thickness was adjusted to satisfy the stability criterion mentioned above. The first node is one half the standard thickness so that the temperature at the wire-charge interface could be computed. Using the base case parameters we determined the time to ignition as a function of initial temperature. The results are shown in Fig. 2 for initial temperatures of 300 K, 100 K, and 10 K which are the approximate temperatures at which initiators have been tested. Ignition is assumed to occur after the first two nodes show a steep rise in temperature. The model predicts that ignition time increases from approximately 1.5 ms at room temperature to 10 ms at 100 K and 27 ms at 10 K.

Tests were performed on initiator samples when they were first qualified for use on the Space Shuttle. The function time was measured by recording the time for the pressure to rise in a closed chamber. The function time was 2 ms at 110 K, and 1 - 3 ms at 10 K for a constant current of 5 A (CC firing mode).<sup>6</sup> The function time was 3 ms at room temperature for a constant firing current of 3.5 A. In some cases the time to "first pressure" and time to maximum pressure were recorded separately, but the latter was identified with the function time of the initiator. The function times in the numerical model corresponds to ignition of the first ZPP node and are thus expected to be smaller than the experimental measurements. Thus the function times predicted by the simple model are too large, but within the expected accuracy. The discrepancy of about an order of magnitude at low temperatures can be attributed to the assumption of constant properties and to errors in assumed property values.

Thermal contact resistance is expected to increase at low temperatures because of differential thermal contraction. The effect of contact resistance is displayed in Fig. 3 which shows the time to ignition for an initial temperature of 10 K and activation energy of  $0.13\Delta H_R$ . Increasing the contact resistance by a factor of 100 to  $10^{-5} \text{ m}^2 \text{ K/W}$  increases the temperature difference between the wire and the charge but reduces the time to ignition. This somewhat surprising result can be explained by noting that the wire heats up much faster when the contact resistance is poor. In this situation the wire acts as a higher temperature source which can heat up the surrounding charge to ignition temperature faster than if the contact resistance is lower. If the contact resistance is increased further to  $10^{-4} \text{ m}^2 \text{ K/W}$  then the bridgewire is almost adiabatic and heats up to melting point within a few milliseconds but the charge does not ignite. In this calculation it is assumed that the wire fuses and no longer carries current once the melting point is reached. The wire subsequently cools down by slow heat transfer to the charge. For the contact resistance and

ORIGINAL PAGE IS  
OF POOR QUALITY

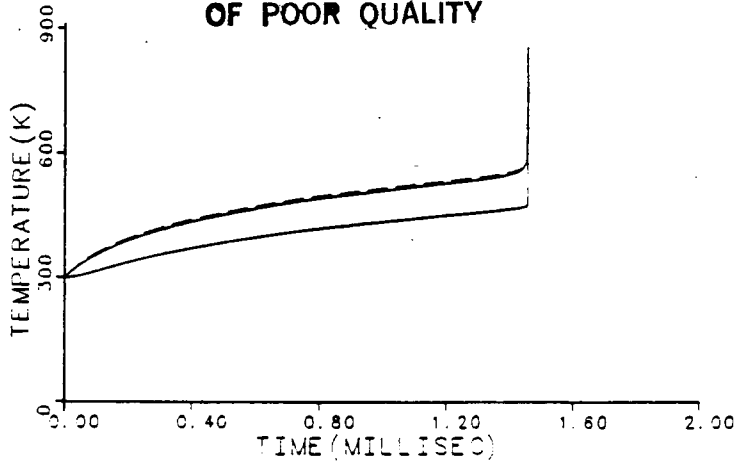
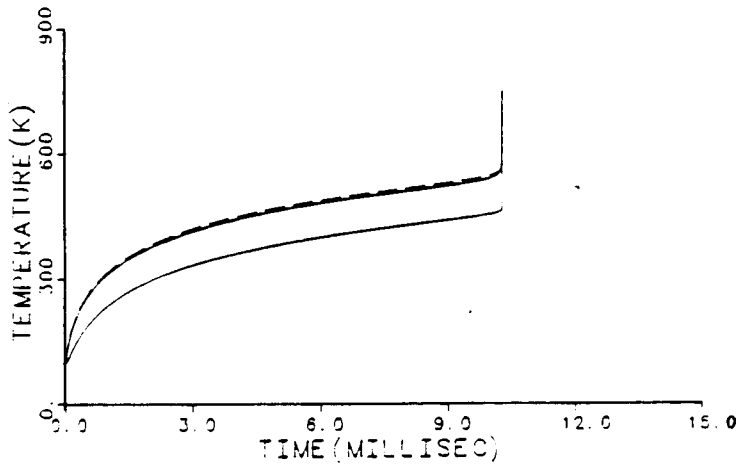
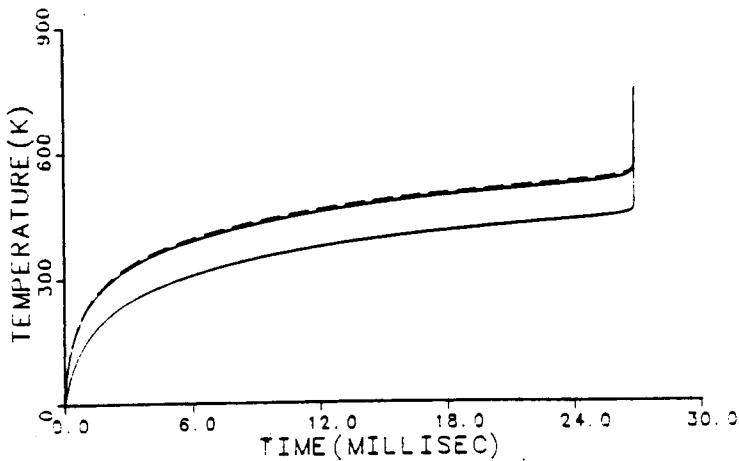


Figure 2. Variation of ignition delay time with initial temperature of the initiator. Dashed line shows wire temperature, solid lines show temperature of the first two nodes in the propellant mixture. Contact resistance:  $10^{-7} \text{ m}^2 \text{ K/W}$  Activation Energy:  $0.13 \Delta H_R$

Initial Temperature: 300 K  
Ignition time = 1.46 ms



Initial Temperature: 100 K  
Ignition time = 10.3 ms



Initial Temperature: 10 K  
Ignition time = 27.0 ms

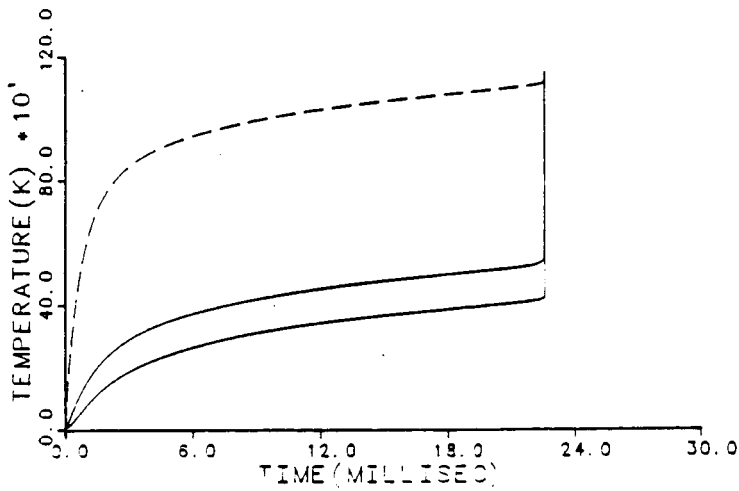
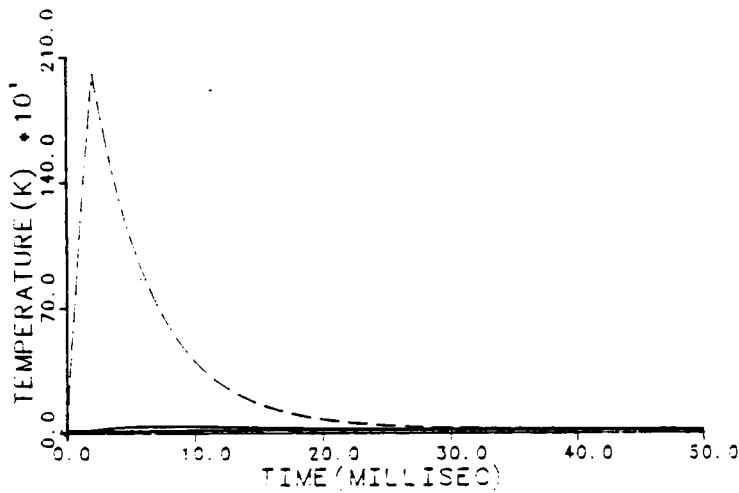
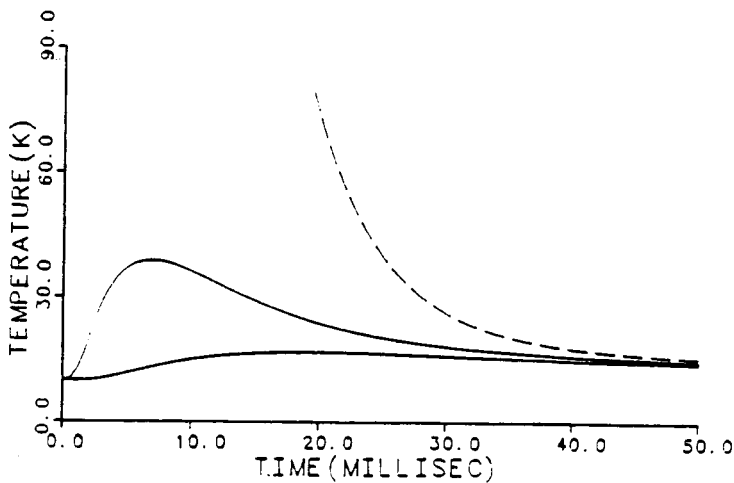


Figure 3. Variation of ignition delay time with thermal contact resistance. Dashed line shows wire temperature, solid lines show temperature of the first two nodes in the propellant mixture. Initial Temperature: 10 K Activation Energy:  $0.13 \Delta H_R$

Contact resistance:  $10^{-5} \text{m}^2\text{K/W}$   
 Ignition time = 22.6 ms



Contact resistance:  $10^{-4} \text{m}^2\text{K/W}$   
 Wire burnout time: 2 ms  
 No ignition



Same as above with expanded ordinate.

ORIGINAL PAGE IS  
OF POOR QUALITY

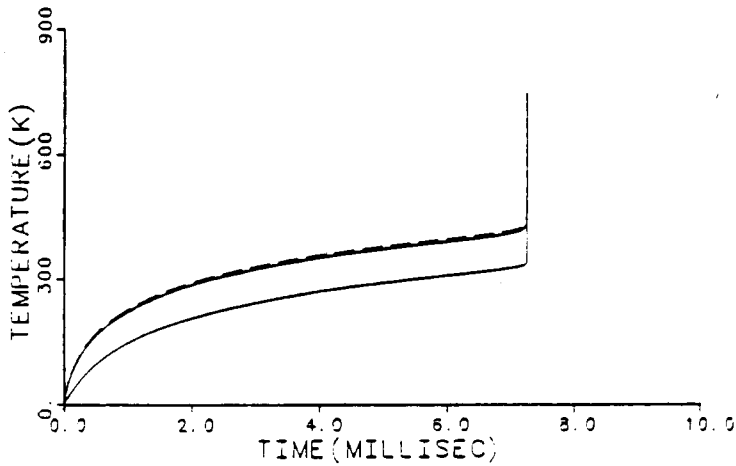
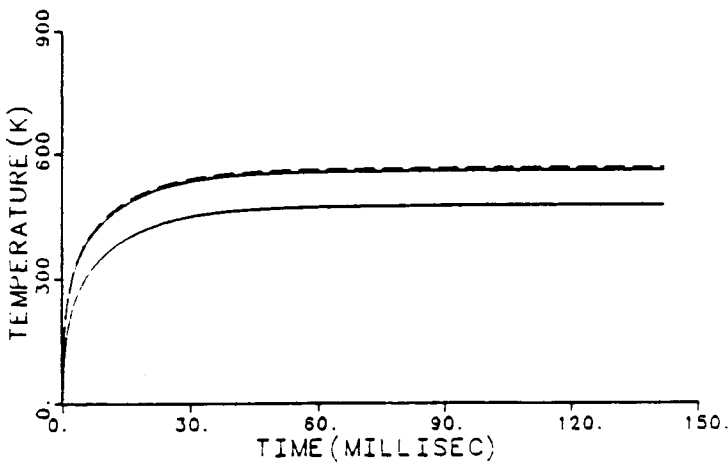


Figure 4. Variation of ignition delay time with activation energy of the propellant. Dashed line shows wire temperature, solid lines show temperature of the first two nodes in the propellant mixture.

Contact resistance:  $10^{-7} \text{m}^2 \text{K/W}$   
Initial Temperature: 10 K

Activation Energy:  $0.10 \Delta H_R$   
Ignition time = 7.25 ms



Activation Energy:  $0.20 \Delta H_R$   
No ignition. System reaches steady state



activation energy chosen for the calculation this heat transfer is insufficient to initiate chemical reaction in the ZPP.

The sensitivity of the model predictions to the activation energy of the charge is shown in Fig. 4 for an initial temperature of 10 K and a contact resistance of  $10^{-7}$  m<sup>2</sup> K/W. When the activation energy is reduced by 30% to  $0.1\Delta H_R$  the model predicts that the time to ignition is reduced by a factor of approximately 3 from 27 ms to 7.3 ms. If the activation energy is increased to  $0.2\Delta H_R$ , the mixture does not ignite at all but approaches steady state. Hence the ignition time is very sensitive to the activation energy of the charge mixture.

The results obtained from this preliminary work showed that even with this simple model ignition time had a non-monotonic dependence on contact resistance and was sensitive to the chemical reaction rate (through the activation energy). However, the function times at low temperature predicted by the model were too large by about an order of magnitude, and it seemed unlikely that useful conclusions could be drawn from the model without additional refinements. In particular, the property data used to model the ZPP mixture were based on extrapolations from similar compounds. It appeared imperative to us that we improve the accuracy of the thermophysical property data on zirconium and potassium perchlorate, and include temperature dependent properties of the other materials if possible.

#### 4.2 Temperature Dependent Material Properties

An extensive literature search was conducted to obtain thermophysical properties of all materials as a function of temperature. The results of the search are summarized in the Appendix. Chemical kinetic data for Zr and KClO<sub>4</sub> mixtures are not available and so the activation energy for the chemical reaction was taken from the Zr/O<sub>2</sub> reaction data<sup>7</sup> and set to 193.1 kJ/mol. The pre-exponential factor for the chemical reaction rate was also modified to  $A = 5.19 \times 10^{25} / \sqrt{T}$  s<sup>-1</sup> and the volumetric energy release rate due to chemical reaction was modelled by

$$\dot{Q} \text{ [W/m}^3\text{]} = \rho \Delta H_R A e^{(-E_a/RT)} = \frac{1.4 \times 10^{36}}{\sqrt{T[\text{K}]}} e^{-23228/T[\text{K}]},$$

where  $\rho$  is the mean mass density of the mixture (4600 kg/m<sup>3</sup>). The sensitivity of the results to the pre-exponential factor and the activation energy were studied parametrically.

During the course of this search we found that the thermal conductivity of alumina is a strong function of temperature (Table 2). At cryogenic temperatures the thermal conductivity of

high purity alumina is 10 times higher than that of ZPP. Thus the alumina charge cup acts as a very effective heat sink at low temperature if the wire makes good thermal contact with it. The thermal conductivity of the alumina is very sensitive to purity. As Table 2 shows, there is a difference of several orders of magnitude between the conductivity of 98% dense alumina and 100% dense alumina. The data were obtained from two different references but their relative consistency is made more credible because the data for sapphire obtained from the two references are in good agreement. Figure 5 presents a comparison of the thermal conductivity of alumina of varying purity. The estimated thermal conductivity of a ZPP mixture is also shown for comparison.

Table 2 Thermal Conductivity of Alumina as a Function of Temperature

T (K)	Thermal Conductivity (W/m K)			
	98% <sup>a</sup>	100% <sup>b</sup>	Sapphire <sup>c</sup>	Sapphire <sup>d</sup>
10	6.7	3000	2600	2901
20	33.1	12500	14600	15700
40		13500	16500	
50	170.8			5192
60		3100	4400	
80		1100	1175	
100	133.1	520	480	452
150		155	150	
200	54.8	80	82	83.7
250		60	58	
300	36.0	42	46	46.1

<sup>a</sup> Ref 8: 99.5% pure, 98% dense, polycrystalline

<sup>b</sup> Ref 9: Pure alumina, 100% dense (probably single crystal)

<sup>c</sup> Ref 9

<sup>d</sup> Ref 8: High purity synthetic, single crystal

We realized that this was a crucial factor that had been neglected in previous analyses, and could explain many of the seemingly contradictory results of experimental measurements. For example, the lack of correlation between measured contact resistance and failure rate could be explained by noting that the bridgewire might be making good thermal contact with the alumina charge cup and not with the charge mixture. The electrothermal response test could not distinguish

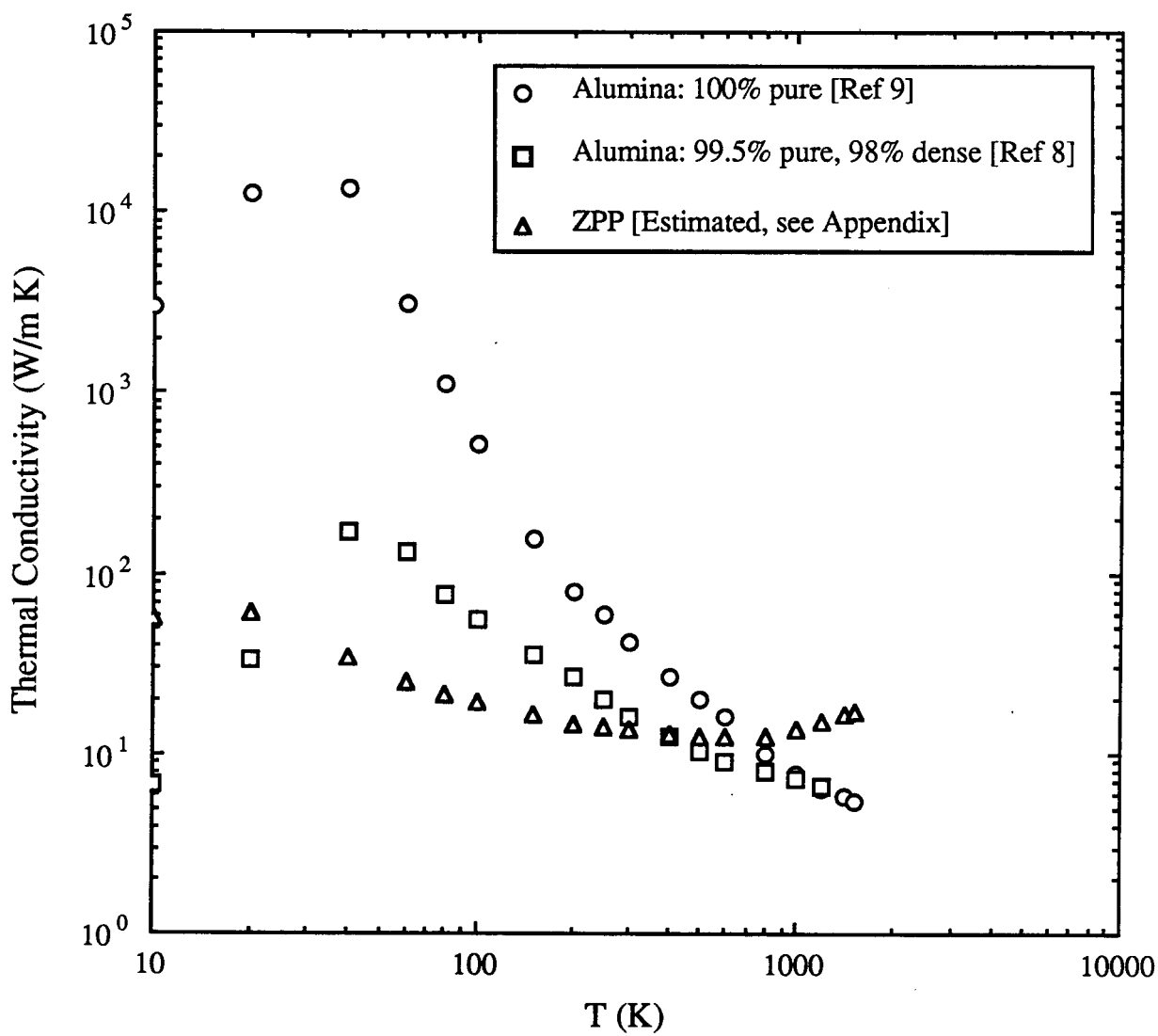


Figure 5 Comparison of the thermal conductivity of various materials as a function of temperature

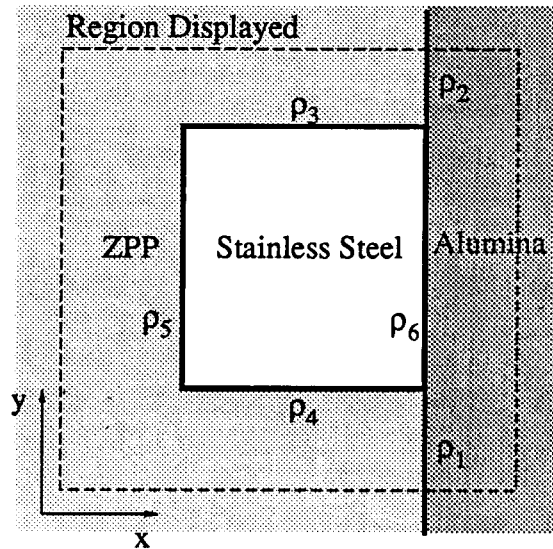
between these two cases. Because of the good thermal contact with the alumina the bridgewire might take as long or longer to burn out, without initiating a reaction in the ZPP. Additionally, heat conduction into the alumina might quench reactions initiated adjacent to the charge cup.

Circumstantial evidence also supports this hypothesis. Initiators from one vendor had a ZPP slurry brushed onto the bridgewire after it was welded to the pins in the charge cup. The slurry was then allowed to dry before pressing the pyrotechnic charge into the cup. Initiators with these “battered” bridgewires were extremely reliable at low temperature, whereas those from another vendor which were not treated in this way were more unreliable.<sup>5</sup> This can be explained by noting the dried slurry would insulate the bridgewire from the alumina charge cup and enhance heat transfer to a reactive mixture.

#### 4.3 Two-dimensional model

A two-dimensional model incorporating temperature dependent thermophysical properties for the various materials was developed. The model allows for the simulation of all three firing modes: the Constant Current (CC), the Standard Firing Unit (SFU), and the Pyrotechnic Initiator Controller (PIC) discussed above. The numerical method used employs the Alternate Direction Implicit (ADI) technique developed by Peaceman and Rachford.<sup>10</sup> This method is unconditionally stable for linear problems. Since the thermophysical properties in this model are temperature dependent, the problem is no longer linear and in some temperature ranges the problem became highly nonlinear because of the strong dependence of the properties on temperature. This caused some instabilities when large time steps were used, but smaller time steps continued to show the needed stability. Small time steps are also needed to maintain adequate accuracy in the calculations.

In the two-dimensional model the cylindrical wire is approximated by a square, and a Cartesian coordinate system was used. Figure 6 shows a portion of the model close to the wire and specifies the  $x$  and  $y$  axis orientations. All calculations were performed per unit length ( $z$ ) of wire and gradients in the  $z$ -direction were neglected. Even though the geometry was distorted, the areas of the various sections (ZPP, wire, and alumina) were chosen to preserve the correct relative masses. Different spatial grid sizes were used to improve the spatial resolution of temperature gradients in the region where the heating is occurring. In the region close to the wire, the grid size was equal to  $4 \mu\text{m}$  in both the  $x$ - and  $y$ - directions. Far away from the wire the grid size was  $193.6 \mu\text{m}$  in the  $y$ -direction in both ZPP and alumina,  $195.1 \mu\text{m}$  in the  $x$ -direction in the ZPP, and  $241.4 \mu\text{m}$  in the  $x$ -direction in the alumina. The mesh had 71 nodes in the  $x$ -direction and 53 nodes in the  $y$ -direction.



$\rho_i$  = Thermal Resistivity ( $\text{m}^2 \text{K/W}$ ) of interface  $i$

Figure 6 Geometry of the two-dimensional model of the NSI.

Several thermal contact resistances are included in the model. The thermal resistivity,  $\rho_i$ , (and hence contact resistance,  $R_i = \rho_i/A_i$ ) of each interface can be specified independently (see Fig. 6). This was done to compute the temperature distribution and performance of the NSI for various combinations of contact resistances between the bridgewire, the charge mixture, and the charge cup.

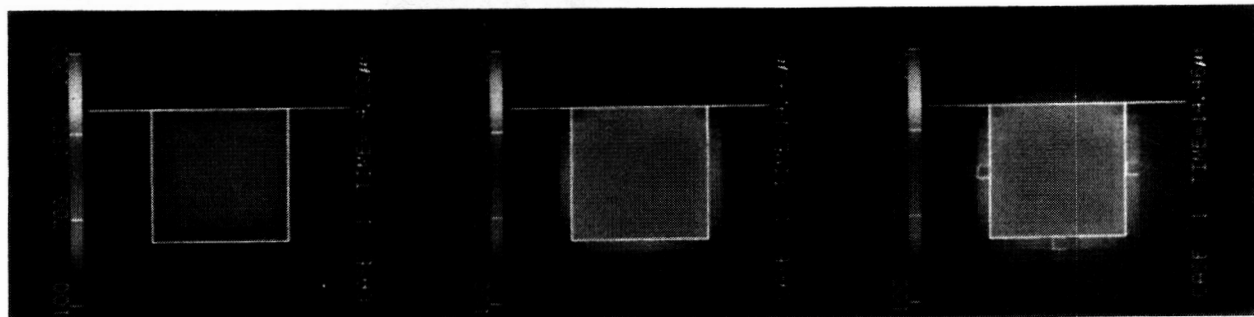
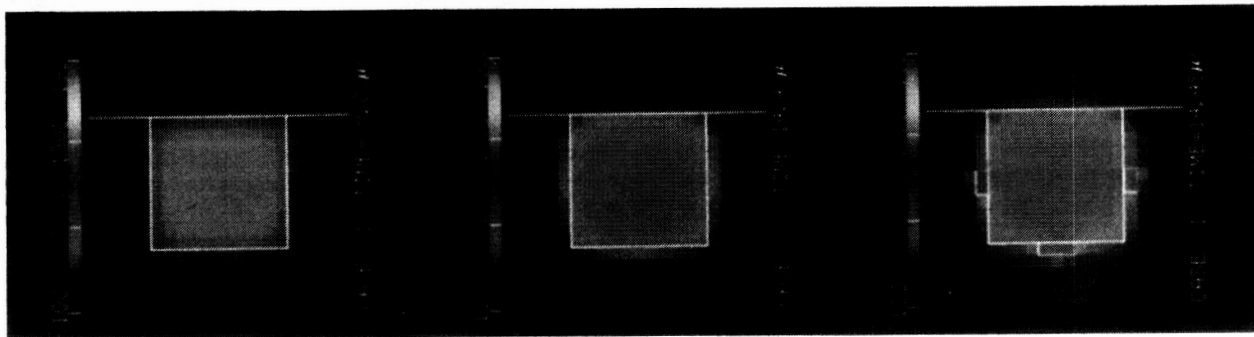
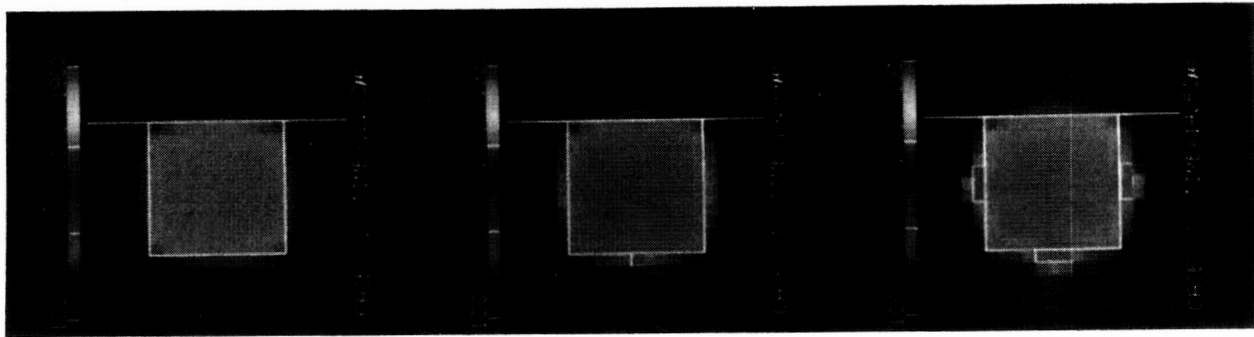
The computational mesh simulating the model geometry was rather large. To improve computational efficiency the code was run to determine the extent of thermal diffusion at the onset of ignition with all the contact resistances set to zero and the initial system temperature at 10 K. This combination of parameters was used because it yields the “worst case” results - maximum energy transfer from the wire to its surroundings and the longest heating time before ignition. The spatial temperature distribution at ignition showed that nodes far away from the wire were unaffected because the thermal diffusion was slow relative to the rate of resistive heating. The nodes outside the “thermal front” were eliminated from the grid in subsequent computations to reduce computing time. The resulting grid had 46 nodes in the  $x$ -direction and 53 nodes in the  $y$ -direction which reduced the number of nodes by about 35%.

Some results obtained using the code are presented in Figs. 7 - 9 which show false color plots of the spatial temperature distribution at various times after firing. The time is noted below each plot. Green represents computed temperatures of 1900 K or above. Only an  $84 \mu\text{m} \times 84 \mu\text{m}$  portion of the computational grid is displayed for greater spatial resolution (see Fig. 6); temperatures outside this region were almost uniform. The computational time step varied during the simulations. It was initially set at 100 ns per sweep (effectively 200 ns time step for the ADI method) and when there was a rapid temperature rise (due to chemical reactions) the time step was reduced to 10 ns (20 ns effective time step). In each case the current through the initiator simulated the PIC firing mode, and the wire and charge were assumed to be at the same initial temperature of 100 K. At this temperature the thermal conductivity of alumina is high but not at its peak. The thermal conductivity used in the simulation corresponds approximately to that of 99.5% pure, 98% dense alumina listed in Table 2.

Figure 7 shows the simulation results for no thermal contact resistance between any of the materials. Ignition first occurs in the ZPP furthest away from the charge cup on the center line of the wire (as expected from symmetry). The computed time to ignition is 14.44  $\mu\text{s}$ ; note the change of time step of the display after 12  $\mu\text{s}$ . The temperature of the alumina adjacent to the bridgewire does not rise as much as the ZPP because heat is conducted away rapidly from the interface. In spite of the differences in thermal conductivity of the materials in contact with the wire, its temperature distribution is almost centro-symmetric, and ignition on the sides of the wire occurs within 20 ns of the first ignition. This indicated that thermal diffusion from the stainless steel bridgewire is the rate limiting process (compare with the results below).

Figure 7 also displays temperature distributions after ignition first occurs; the rapid spread of ignition into the adjacent charge can be seen. The extent of chemical reaction at each grid point is monitored and the energy release is limited to the consumption of the initial quantity of charge at that location. However, the phase changes that accompany the large heat release due to the chemical reactions are not modelled. The reacted zone is modelled as a very hot solid (temperatures reach  $\sim 15,000$  K) with the specific heat and thermal conductivity of the original ZPP. Changes in the thermal transport properties corresponding to formation of  $\text{ZrO}_2$  and  $\text{KCl}$  are neglected. Thus the calculations of the chain reaction after the first ignition are very qualitative. The product temperature is much too high because phase changes are not modelled and the enthalpy of vaporization is not accounted for when computing product temperature. However, the calculations of the rate of propagation of the reaction are likely to be conservative, since the hot gaseous products of the chemical reaction will expand rapidly through the voids in the charge mixture. This will increase the speed of propagation of the reaction compared to thermal diffusion.

Figure 7 Temperature distribution in initiator as a function of time.  
Initial temperature = 100 K,  $\rho_i = 0, i = 1, \dots, 6$ .



ORIGINAL PAGE IS  
OF POOR QUALITY

ORIGINAL PAGE  
COLOR PHOTOGRAPH

Figure 8 illustrates the effect of thermal contact resistance on the initiator response. In this case  $\rho_i = 10^{-6} \text{ m}^2 \text{ K/W}$ ,  $i = 1, \dots, 5$  (ZPP/ $\text{Al}_2\text{O}_3$ , ZPP/SS) and  $\rho_6 = 10^{-5} \text{ m}^2 \text{ K/W}$  ( $\text{Al}_2\text{O}_3$ /SS). The ZPP charge is heated to ignition rapidly, while the alumina temperature does not appear to change significantly. This occurs because the relatively high contact resistance between the heated wire and the charge cup inhibits heat transfer to the alumina, and the heat that is transferred is rapidly conducted away from the interface. In this case ignition first occurs 20.44  $\mu\text{s}$  after firing on the sides of the wire adjacent to the alumina. This indicates that inhibition of heat transfer into the alumina creates a non-uniform temperature distribution in the wire though the temperature differences cannot be resolved visually in the figure. The wire side away from the charge cup is slightly cooler and the charge adjacent to it ignites about 60 ns later. Because of the exponential dependence of the rate of chemical reaction on temperature, the pyrotechnic charge goes from ignition temperature  $\sim 600 \text{ K}$  (strawberry pink) to above 1900 K (green) within one time step (20 ns).

Figure 9 shows the case when the contact resistance values are reversed from the previous case. Here  $\rho_i = 10^{-5} \text{ m}^2 \text{ K/W}$ ,  $i = 1, \dots, 5$  (ZPP/ $\text{Al}_2\text{O}_3$ , ZPP/SS) and  $\rho_6 = 10^{-6} \text{ m}^2 \text{ K/W}$  ( $\text{Al}_2\text{O}_3$ /SS). In this case the initiator fails because the wire melts before appreciable heating of the ZPP occurs. The heat transfer to the alumina immediately adjacent to the wire does not raise its temperature very much, because of its high thermal conductivity at low temperature. The influence of the thermal conductivity difference can be seen by comparing the (false) color temperature of the ZPP at 20  $\mu\text{s}$  in Fig. 8, with the color temperature of the alumina at 22  $\mu\text{s}$  in Fig. 9. The former is considerably hotter (after a slightly shorter time and with a cooler bridgewire) than the latter. The melting temperature of stainless steel is 1700 K (yellow-green) and the wire burns out 32.6  $\mu\text{s}$  after firing. This should be compared to a bridgewire burnout time of 28.4  $\mu\text{s}$  obtained if the contact resistances were so high that the wire were essentially adiabatic. The overall contact resistance in this case is 2.4 times larger than the previous case; the power transfer coefficient ( $\gamma$ ) measured in an ETR test (see section 3) would be only 2.4 times lower in this case but the difference in performance is very significant.

The poor correlation between initiator performance and power transfer coefficient was investigated further. The thermal resistivity  $\rho_6$  was reduced by a factor of 10 to  $10^{-7} \text{ m}^2 \text{ K/W}$  while the other resistivities were maintained at  $10^{-5} \text{ m}^2 \text{ K/W}$ . The initiator failed as in the previous case and the bridgewire burnout time did not change within the accuracy of the calculation (effective time step 200 ns). The value of the power transfer coefficient in this case is more than



ORIGINAL PAGE  
COLOR PHOTOGRAPH

Figure 8

Temperature distribution in initiator as a function of time.

Initial temperature = 100 K,  $\rho_i = 10^{-6} \text{ m}^2 \text{ K/W}$ ,  $i = 1, \dots, 5$ ;  $\rho_6 = 10^{-5} \text{ m}^2 \text{ K/W}$

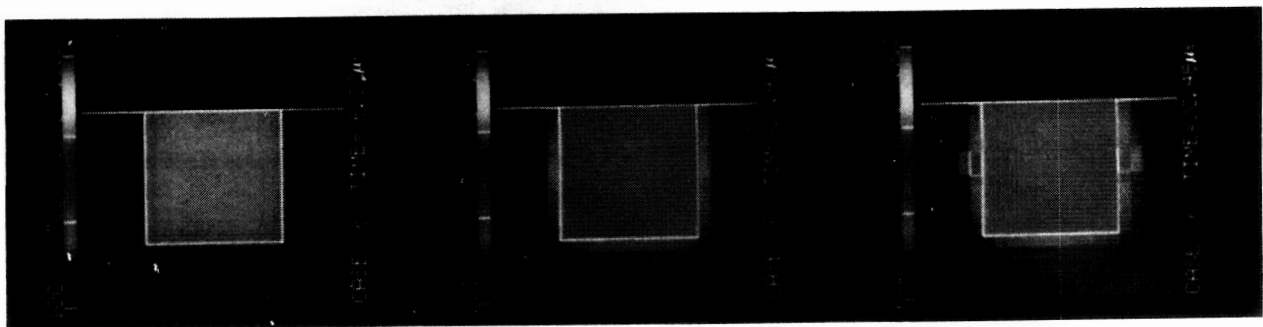
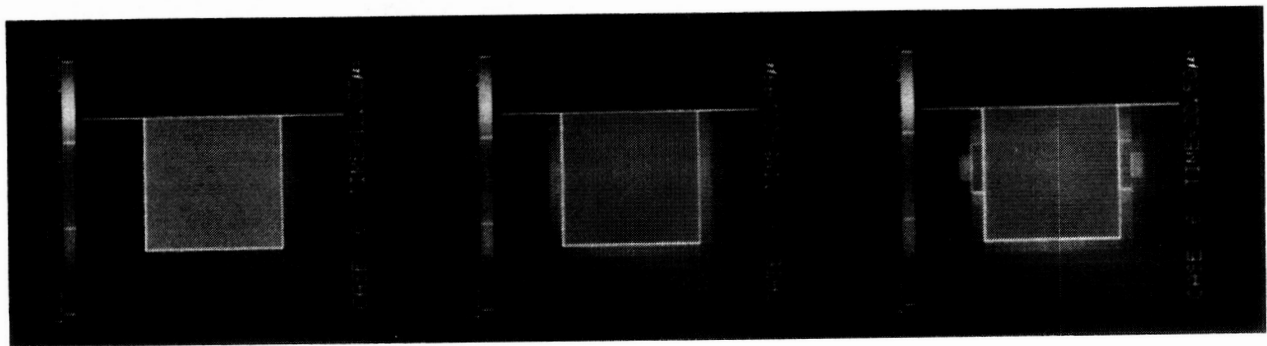
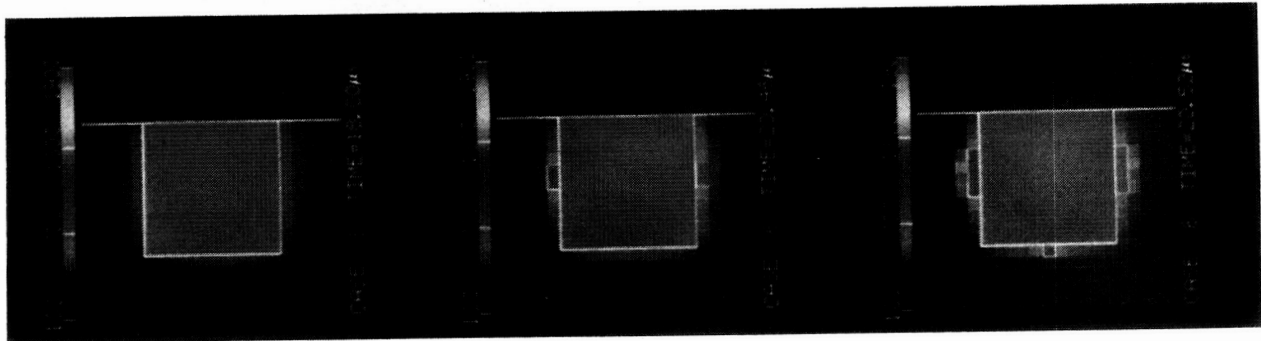
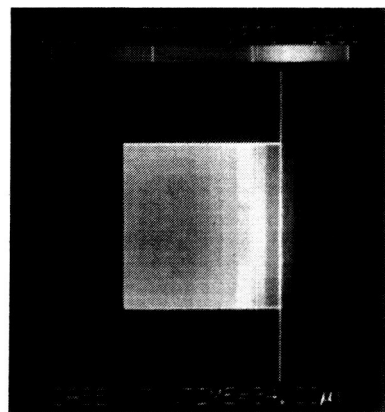
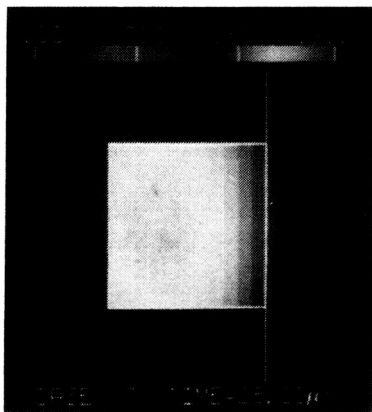
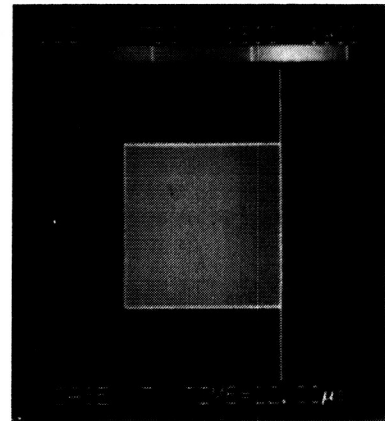
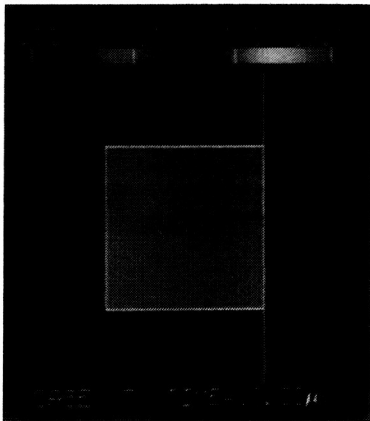
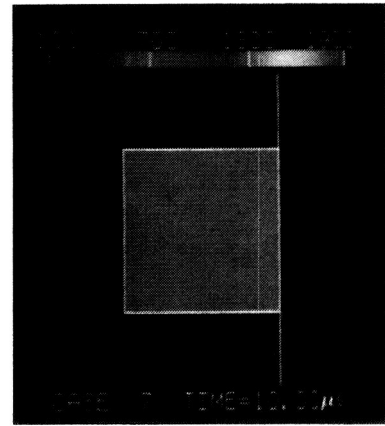
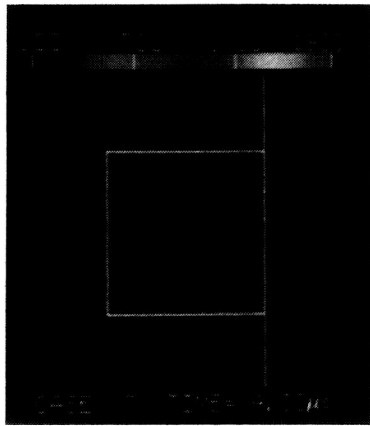


Figure 9

Temperature distribution in initiator as a function of time.

Initial temperature = 100 K,  $\rho_i = 10^{-5} \text{ m}^2 \text{ K/W}$ ,  $i = 1, \dots, 5$ ;  $\rho_6 = 10^{-6} \text{ m}^2 \text{ K/W}$



three times *greater* than the case when the initiator fired successfully (Fig. 8). Thus the modelling proves that initiator performance does not correlate with power transfer coefficient. This parameter does not discriminate the material to which the bridgewire is transferring energy. Energy transferred to the alumina at low temperature is rapidly conducted away and does not assist in ignition of the pyrotechnic charge. Because of the relatively large thermal capacity of the alumina it does not get hot enough to ignite the pyrotechnic mixture indirectly.

## 5. CONCLUSIONS

The results obtained show that changes in the contact resistance of less than a factor of 10 can make the difference between successful firing and failure. Initiators with bridgewires which make excellent thermal contact with the alumina but poor contact with the ZPP will fail even though they have better total heat transfer coefficients. Measurements of overall heat transfer from the wire do not account for the material into which the energy is transferred. Thus they are not reliable predictors of performance.

The modelling suggests manufacturing and/or design changes that will improve the reliability of initiators. Improving the thermal contact between the bridgewire and the pyrotechnic charge by “buttering” the bridgewire during manufacture will improve reliability. The bridgewire should not be stretched tightly across the connecting pins before welding, because differential contraction might draw it closer to the charge cup and improve thermal contact with it at low temperature.

A design change to reduce thermal conduction from bridgewire to the charge cup at low temperature would also improve reliability. The simplest means of accomplishing this is to reduce the thermal conductivity of the alumina at cryogenic temperatures. Since the thermal conductivity is very sensitive to packing density and impurities (see Fig. 5), the charge cup could be made from alumina with lower purity. The alumina presently used must meet or exceed certain density and purity specifications and is about 98% pure, 100% dense.<sup>11</sup> If the specifications are changed so that there is a *maximum* density and/or purity the thermal conductivity at low temperatures could be significantly reduced without compromising mechanical properties. This design modification has the advantage of using a cheaper material for the charge cup although this is unlikely to affect the overall cost of the initiator significantly.

If alumina with low enough thermal conductivity at low temperature is used for the charge cup it may permit discrimination of failure-prone initiators using the ETR test described in Section 3. The test will identify those initiators which do not make good thermal contact with the pyrotechnic mixture provided that the conductivity of the charge cup is much lower than the pyrotechnic charge.

The numerical model developed in this work will be refined to simulate initiator performance as accurately as possible and will be used to test the proposed design changes.

6. REFERENCES

- 1 "NASA Standard Initiator Failure Analysis Report", *Preliminary*, T. J. Graves (ed.) National Aeronautics and Space Administration, Lyndon B. Johnson Space Center, Houston, Texas, February, 1987.
- 2 Ref. 1, Appendix A.
- 3 S. Kakac and Y. Yener, *Heat Conduction*, p 318, Hemisphere, New York, 1985
- 4 Ref. 1, Appendix N.
- 5 Ref. 1, Appendix Q
- 6 Ref. 1, Appendix C.
- 7 J. Belle and M. W. Mallett, "Kinetics of the High Temperature Oxidation of Zirconium", *J. Electrochem. Soc.* **101**, p. 339, (1954).
- 8 K. Wefers and G. M. Bell, "Oxides and Hydroxides of Aluminum", Technical Paper No. 19, Alcoa Research Laboratories, 1972.
- 9 *Heat Exchanger Design Handbook*, p. 5.5.6-2, Hemisphere Publishing Corporation, Washington, 1983.
- 10 B. Carnahan, H. A. Luther, and J. O. Wilkes, *Applied Numerical Methods*, Wiley, New York, 1973.
- 11 K. van Tassel, private communication.
- 12 S. S. Todd, "Heat Capacities of Zirconium, Zirconium Nitride, and Zirconium Tetrachloride", *Am. Chem. Soc. J.* **72**, p. 2914, 1950.
- 13 M. W. Chase, Jr., C. A. Davies, J. R. Downey, Jr., D. J. Frurip, R. A. McDonald, A. N. Syverud, *J. Phys. Chem. Ref. Data* **14**, Supplement No.1, JANAF Thermochemical Tables, Third Edition, p. 757, (1985).
- 14 Y. S. Touloukian, "Thermophysical Properties of Matter", vol. 2, p 647, Plenum Publishing Corporation, 1970.
- 15 G. T. Furukawa, T. B. Douglas, R. E. McCoskey, D. C. Ginnings, "Thermal Properties of Aluminum Oxide from 0-1200 K", *J. Res. Nat. Bur. Stand.* **57**, pp. 67-82, 1956.
- 16 Y.S. Touloukian, "Thermophysical Properties of Matter" vol. 2, p. 119, Plenum Publishing Corporation, 1970.
- 17 Y.S. Touloukian, "Thermophysical Properties of Matter", vol. 4, pp. 699-708, Plenum Publishing Corporation, 1970.
- 18 Y.S. Touloukian, "Thermophysical Properties of Matter", vol. 1, p. 1175, Plenum Publishing Corporation, 1970.

## APPENDIX

### CURVEFITS TO THERMOPHYSICAL PROPERTIES

Curvefits to the thermophysical properties of Zr, KClO<sub>4</sub>, Al<sub>2</sub>O<sub>3</sub>, and SS 304 obtained from several references were used in the simulation of the NSI. The equations are listed below.

#### Zirconium (Zr)

##### Specific Heat<sup>12</sup> (J/Kg K)

$$10 < T < 300 \text{ K} \quad c_p = -1.093 \cdot 10^{-9} T^5 + 8.767 \cdot 10^{-7} T^4 - 2.360 \cdot 10^{-4} T^3 + 0.0187 T^2 + 1.7661 T - 0.88$$

$$300 < T < 1100 \text{ K} \quad c_p = 3.091 \cdot 10^{-7} T^3 - 6.207 \cdot 10^{-4} T^2 + 0.489 T + 186.51$$

$$T > 1100 \text{ K} \quad c_p = 395$$

##### Thermal Conductivity<sup>9</sup> (W/m K)

$$10 < T < 40 \text{ K} \quad k = -0.1117 T^2 + 4.25 T + 67.67$$

$$40 < T < 300 \text{ K} \quad k = 286.8429 T^{-0.4552}$$

$$300 < T < 1500 \text{ K} \quad k = -1.219 \cdot 10^{-8} T^3 + 4.389 \cdot 10^{-5} T^2 - 0.0401 T + 31.61$$

$$T > 1500 \text{ K} \quad k = 25$$

#### Potassium Perchlorate (KClO<sub>4</sub>)

##### Specific Heat<sup>13</sup> (J/Kg K)

$$10 < T < 260 \text{ K} \quad c_p = -5.066 \cdot 10^{-8} T^4 + 9.424 \cdot 10^{-5} T^3 - 0.0435 T^2 + 8.9371 T - 77.16$$

$$260 < T < 1500 \text{ K} \quad c_p = 1.335 \cdot 10^{-12} T^5 - 6.802 \cdot 10^{-9} T^4 + 1.362 \cdot 10^{-5} T^3 - 0.0136 T^2 + 7.3602 T - 480.58$$

$$T > 1500 \text{ K} \quad c_p = 1600$$

##### Thermal Conductivity<sup>14</sup> (W/m K)

No data on the thermal conductivity of KClO<sub>4</sub> was found. It was assumed to be approximately that of KNO<sub>3</sub>.

$$k = 1.0 \text{ for all } T$$

## Alumina (Al<sub>2</sub>O<sub>3</sub>)

### Specific Heat<sup>15</sup> (J/Kg K)

$$10 < T < 200 \text{ K} \quad c_p = 4.643 \cdot 10^{-9} T^5 - 2.727 \cdot 10^{-6} T^4 + 5.047 \cdot 10^{-4} T^3 - 0.0177 T^2 + 0.249 T - 0.89$$

$$200 < T < 1200 \text{ K} \quad c_p = 2.927 \cdot 10^{-12} T^5 - 1.259 \cdot 10^{-8} T^4 + 2.168 \cdot 10^{-5} T^3 - 0.019 T^2 + 8.9272 T - 676.76$$

$$T > 1250 \text{ K} \quad c_p = 1250$$

### Thermal Conductivity<sup>8,16</sup> (W/m K)

$$10 < T < 50 \text{ K} \quad k = 0.049 T^2 + 1.176 T - 9.94$$

$$50 < T < 150 \text{ K} \quad k = -0.0038 T^2 - 0.1932 T + 190.4$$

$$150 < T < 1200 \text{ K} \quad k = 3.476 \cdot 10^4 T^{-1.2098}$$

$$T > 1200 \text{ K} \quad k = 6.5$$

## Stainless Steel 304

### Specific Heat<sup>17</sup> (J/Kg K)

$$10 < T < 1070 \text{ K} \quad c_p = -2.064 \cdot 10^{-12} T^5 + 5.319 \cdot 10^{-9} T^4 - 4.2 \cdot 10^{-6} T^3 + 3.962 \cdot 10^{-4} T^2 + 0.9225 T + 220.22$$

$$T > 1070 \text{ K} \quad c_p = 595$$

### Thermal Conductivity<sup>18</sup> (W/m K)

$$10 < T < 1660 \text{ K} \quad k = 3.952 \cdot 10^{-14} T^5 - 1.816 \cdot 10^{-10} T^4 + 3.108 \cdot 10^{-7} T^3 - 2.432 \cdot 10^{-4} T^2 + 0.0991 T + 0.88$$

$$T > 1500 \text{ K} \quad k = 34.7$$